Hindawi Publishing Corporation
Journal of Materials
Volume 2016, Article ID 1285721, 9 pages
http://dx.doi.org/10.1155/2016/1285721

Research Article

Synthesis and Characteristics of Valeric Acid-Zinc Layered Hydroxide Intercalation Material for Insect Pheromone Controlled Release Formulation

Rozita Ahmad,[1,2] Mohd Zobir Hussein,[1] Siti Halimah Sarijo,[3] Wan Rasidah Wan Abdul Kadir,[2] and Taufiq-Yap Yun Hin[4]

[1]*Material Synthesis and Characterization Laboratory (MSCL), Institute of Advanced Technology (ITMA), Universiti Putra Malaysia (UPM), 43400 Serdang, Selangor, Malaysia*
[2]*Forest Biotechnology Division, Forest Research Institute Malaysia (FRIM), 52109 Kepong, Selangor, Malaysia*
[3]*Faculty of Applied Science, Universiti Teknologi MARA (UiTM), 40540 Shah Alam, Selangor, Malaysia*
[4]*Chemistry Department, Faculty of Science, Universiti Putra Malaysia (UPM), 43400 Serdang, Selangor, Malaysia*

Correspondence should be addressed to Mohd Zobir Hussein; mzobir@upm.edu.my

Received 22 June 2016; Accepted 7 September 2016

Academic Editor: Yulin Deng

A new intercalation compound of insect pheromone, valeric acid (VA), based on zinc layered hydroxide (ZLH) as host release material, was successfully prepared through coprecipitation method. The as-produced organic-inorganic nanolayered material, valerate nanohybrid, VAN, shows the formation of a new peak at lower 2θ angle with basal spacing of 19.8 Å with no ZnO reflections, which indicate that the intercalation of anion between the inorganic ZLH interlamellae was accomplished. The elemental, FTIR, and ATR analyses of the nanohybrid supported the fact that the intercalation with the percentage anion loading was calculated to be 23.0% (w/w). The thermal stability property of the resulting nanohybrid was enhanced compared to the unbound anion. Field emission scanning electron micrograph of the ZnO has a nonuniform granular structure but transforms into flake-like structure with various sizes after the intercalation process. Release kinetics of anion from the interlayer of intercalated compound exhibited a slow release behavior governed by the pseudo-second-order kinetic model at different pHs of aqueous media. The valerate anion was released from VAN with the highest release rate at pH 4. These findings provide the basis to further development of controlled release formulation for insect pheromone based on ZLH intercalation.

1. Introduction

Controlled release materials acting as host and delivery system for many active ingredients such as drugs, fertilizers, pesticides, and cosmetic agents have gained high interest due to their multiple functionalities. These include protecting the active agents from degradation, increase stability of the chemical, and prevent loss through leaching or evaporation and prolonged activity duration of an active agent. Furthermore, they prevent an active agent from direct contact with human or surroundings and reduce multiple application which promotes safe environment.

The use of pheromone as alternative to chemical insecticide was reported to be one of the potential biopesticides for insect control [1]. However, the environmental factors such as heat, sunlight, and rainfall could affect the pheromone release. Insect pheromone contains volatile compounds and is unstable due to degradation and isomerization at ambient temperature or in the presence of light [2]. Thus, a suitable encapsulated material is required to minimise the environmental related problem.

Intense research has been carried out in employing layered metal hydroxide (LMH) as controlled release formulations for various applications such as herbicide [3], flame retardant [4], UV absorbers [5], drug carrier [6], and anticorrosion agent [7] due to anion exchangeable reactions. Layered metal hydroxides compounds can be classified into three groups based on their formula structure. They are layered double hydroxides (LDH), hydroxyl double salts (HDS), and layered hydroxide salt (LHS). LDH is

group of compounds comprised of two metal cations, either one monovalent or one divalent and one trivalent cations. LDH can be expressed by the general formula, $[M^{2+}_{1-x}M^{3+}\,x(OH)_2]^{x+}\,(A^{m-})_{x/m}{\cdot}nH_2O$. HDS contain two types of divalent metal cations and the composition is expressed as $[(M^{2+}_{1-x}Me^{2+}_{1+x})(OH)_{3(1-y)}]A^{m-}_{(1+3y)/m}\cdot nH_2O$. LHS is also known as layered single-metal hydroxide group which consists of only one type of divalent metal cation and is represented by $M^{2+}(OH)_{2-x}(A^{n-})_{x/n}\cdot nH_2O$, where M^{2+} denotes the divalent metallic cations such as Mg^{2+}, Zn^{2+}, Ni^{2+}, Cu^{2+}, Mn^{2+}, and Co^{2+} and M^{3+} represents the trivalent metallic cations such as Al^{3+}, Fe^{3+}, Co^{3+}, and Cr^{3+}. A^{m-} is interlayer anions that can be organic or inorganic molecules with negative charge and m neutralizes the positive charge of the cations.

Zinc layered hydroxide (ZLH) is a type of LHS, comprised of zinc as the metal cation in which only zinc and hydroxyl represent the inorganic layers. ZLH structure is comprised of 2 parts: positively charged brucite-like inorganic layers and exchangeable anions and water molecules in the interlayer. The positively charged inorganic layer is electrically balanced by the negative charged anions and water molecules enable the accommodation of functional anion between the interlayer regions. The stacking layers of ZLH interlaying with anionic layers can form a nanocomposite material with high stability and controllable functionalities [8]. The interlayer anions can be exchanged with various organic and inorganic charged compounds. ZLH is an interesting host nanomaterial due to the fact that its anion exchange ability has led to the formation of various nanocomposite materials in multiple applications such as catalyst host [9], surfactant nanomaterial [10], and sensors and photoelectrical devices [11].

Intercalation of anion between the interlayer spacings of ZLH can be achieved using various techniques. There are various methods reported for the preparation of ZLH nanohybrid such as urea hydrolysis [12], pulse laser-ablation technique [10], exfoliation-restacking route method [9], and chemical bath deposition [13]. Coprecipitation technique which is among the simple synthesis methods that employ less chemical with fewer preparation steps has been frequently adopted in the ZLH nanocomposite synthesis [14, 15]. Furthermore, this method uses normal laboratory equipment and no dedicated complex instrumental setup is required. In anion exchange method, the ZLH matrices need to be preprepared into solid form before mixing with the active agent [16]. The coprecipitation methods have been studied in the synthesis of ZLH nanohybrid as carrier for herbicides [17, 18], drugs [19], and UV-absorber [20, 21].

To date, research on ZLH as nanocarrier for insect pheromone has not yet been reported elsewhere. Due to this reason and relatively few works reported for nonaromatic or aliphatic carboxylic acid type [22, 23], we have chosen valeric acid (VA), an insect pheromone with low melting point existing in colorless liquid to be intercalated into ZLH, and discuss our investigation here. Valeric acid, a linear carboxylic compound as guest anion, was intercalated into the interlayer region of the ZLH as a host material by coprecipitation method for the formation of a two-dimensional organic-inorganic nanohybrid structure, VAN. Furthermore, to the best of our knowledge no such work on the intercalation of liquid pheromone into any ZLH has been accomplished, and therefore it is worth looking into. In this study, we report the physicochemical properties of the resulting nanohybrid VAN and further investigate the release behavior of valerate anions into the aqueous media at various pHs.

2. Experimental

2.1. Synthesis of Nanohybrid. All chemicals used in this experiment were obtained from various chemical suppliers and used without any further purification. All solutions were prepared using deionized water. About 0.10 g of ZnO was suspended into 100 mL deionized water and was stirred on a magnetic stirrer for 15 minutes. Valeric acid solution (0.5 M) was prepared by mixing 5.60 mL in 20 mL ethanol and adjusted to 100 mL with deionized water in a volumetric flask. The VA solution was then added dropwise into ZnO suspension with constant stirring, producing a clear mixed solution. pH of the solution was adjusted to 7.9 using 0.5 M NaOH aqueous solution to obtain white precipitate. The slurry solution was vigorously stirred using a magnetic stirrer for 3 h at room temperature and continued for 18 h at 70°C. The as-synthesized product was centrifuged, thoroughly washed with deionized water, and dried in an oven at 70°C. The resulting material was ground into fine powder for further use and characterization.

2.2. Characterization. Powder X-ray diffraction patterns of the nanohybrid were obtained at 2–60° on a Shimadzu Diffractometer XRD-6000 using CuK_α radiation (λ = 1.5418 Å) and dwell time of 4 degrees per minute. Fourier transform infrared (FTIR) spectra were recorded over the range of 400–4000 cm^{-1} on a Perkin Elmer 1725X Spectrophotometer using the KBr disc method. Attenuated total reflectance (ATR) method was employed on a Perkin Elmer Spectrum 100 FTIR Spectrometer to determine the functional groups present in valeric acid, since it is liquid in nature. The carbon and hydrogen composition was analysed by a CHNS analyzer, model Thermofinnigan Flash 2000 series. The amount of Zn in the sample was extracted with mineral acids and its concentration was determined by a Varian 725-OES inductive coupled plasma optical emission spectrometer. Thermogravimetry and differential thermogravimetry measurements were recorded using a Mettler Toledo instrument at heating rate of 10°C/minute in the range of 28–1000°C. The surface morphology analysis of the synthesized nanohybrid was captured on a field emission scanning electron microscope, model JEOL JSM-7600.

3. Controlled Release Study

The controlled release study of VA from the nanohybrid into the aqueous media was determined by distilled water at pHs 4, 6.5, and 8. The pH was adjusted by either HCl or NaOH. About 2 mg of the intercalated compound was placed in a cuvette containing 3.5 mL of aqueous solution. The study was carried out *in situ* in which the accumulated

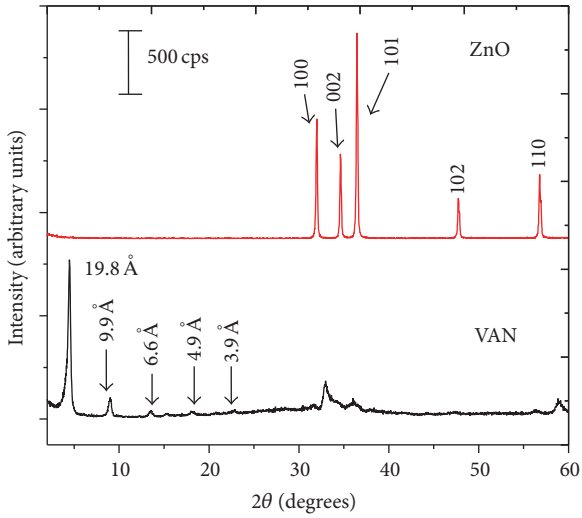

Figure 1: PXRD patterns of ZnO and the nanohybrid VAN prepared at 0.5 M VA.

amount of VA released is automatically recorded at every 30 seconds at λ_{max} 205 nm using a Perkin Elmer UV-Visible Spectrophotometer, Lamda 35. The analysis was done continuously until the equilibrium stage was achieved. The data of the release was fitted to pseudo-first order, pseudo-second order, and parabolic diffusion kinetics models. All the aqueous media and Zn^{2+} from ZnO solution have no interference at λ_{max} 205 nm. After the controlled release, the pH 4, 6.5, and 8 solutions were filtered through Whatman filter paper number 2. The filtrate was analysed using ICP-OES to determine Zn^{2+} content to detect dissolution of ZLH layer from VAN.

4. Results and Discussion

4.1. Powder X-Ray Diffraction and Surface Morphology. Figure 1 shows the PXRD patterns for zinc oxide and VAN. ZnO exhibits a distinctive pattern with five sharp reflections at 2θ = 30–60° region, corresponding to 100, 002, 101, 102, and 110 lattice planes which indicate high crystallinity of the precursor. Previous studies of ZLH intercalated with nitrate ions show sharp diffraction peak with basal spacing of 9.6–9.9 Å recorded around 2θ = 9.3 due to the 200 planes of the monoclinic structure [24, 25]. The basal reflections of VAN are shifted to lower 2θ with d-spacings of 19.8 Å, 9.9 Å, and 6.6 Å. This indicated that intercalation of valerate anion into interlayer space of ZLH has occurred. The evenly d-spacing values of these reflection peaks with ratio of 1, 2, and 3, respectively, indicated a well formation and orderly stacked interlayer of the new nanohybrid VAN. The absence of the intense peaks of ZnO phase suggested that VAN is a pure phase, in which the ZnO phase was completely transformed to ZLH [26] and evident to the successful intercalation of the guest anion, valeric acid has been accomplished. The surface morphologies for ZnO and VAN are presented in Figure 2. Zinc oxide has a nonuniform granular structure without any specific shapes. The formation of VAN resulted in a morphology transformation into nonuniform flaky shapes with no specific structures.

Table 1: ATR and FTIR absorption bands with functional group assignment for VA and VAN.

Assignments	VA	VAN
ν (O-H)	—	3380
ν (CH_2)	2964	2957
ν (C=O) in COOH	1712	—
ν_{asym} (COO^-)	—	1545
ν (C-O) in carboxylic group	1362	1370
δ (O-H)	1222	—
ν (C-O) in carboxylic group	1093	—
Stretching (C-O) in COO^-	—	1013

4.2. Spatial Orientation of Guest Anion between ZLH Interlayers. Intercalation of the guest anion between the metal hydroxide layers resulted in an increase of basal spacing due to the dimension and spatial arrangement of the organic moiety in the interlamellae of host material, ZLH. The dimensional size of VA was determined using the Chemoffice Software Ultra, 2008, 11.01. Figure 3(a) shows the three-dimensional molecular size of VA with x-, y-, and z-axis to be 7.2, 8.7, and 4.9 Å, respectively. Using the average basal spacing of 19.8 Å for VAN obtained from PXRD study, the interlayer space for anion can be estimated. With the thickness of ZLH layer being 4.8 Å [26] and 2.6 Å for each zinc tetrahedron, the gallery space available is calculated to be 9.8 Å. Therefore, the suggested spatial orientation for the VA anion between the ZLH interlayers as bilayer arrangement is illustrated in Figure 3(b). The gallery space of 9.8 Å permits two VA anions to be positioned superimposed from z-axis and arranged in bilayer stacking. This fitted nicely twice the thickness of VA molecules, 4.9 Å.

4.3. FTIR and ATR Spectroscopy. FTIR spectra for ZnO and VAN synthesized using 0.5 mol/L VA are shown in Figures 4(a) and 4(b), respectively. The absorption bands for valeric acid and its nanohybrid VAN are highlighted in Table 1. FTIR spectra of ZnO in Figure 3(a) showed a single strong band at 376 cm^{-1} due to the vibration of zinc and oxygen sublattices [27]. ATR spectrum of VA in Figure 4(c) portrayed a sharp band at 1712 cm^{-1} due to the C=O stretching of the carboxylic group.

Valeric acid also exhibits two other intense peaks recorded at 1362 and 1222 cm^{-1} which are attributed to C-O of carboxylic bond and OH bending [28], respectively. A weak band observed at 2964 cm^{-1} can be assigned to CH_2 stretching of the methylene group of linear-chain carboxylic acids.

The FTIR spectrum of VAN depicted in Figure 4(b) showed that most of the vibrations are similar to the free anion VA (Figure 4(c)). However, due to the intercalation process, some of the peaks in VAN are observed to be slightly shifted from the original position of pure VA as a result of the interaction process of VA anion into the ZLH interlayer. This

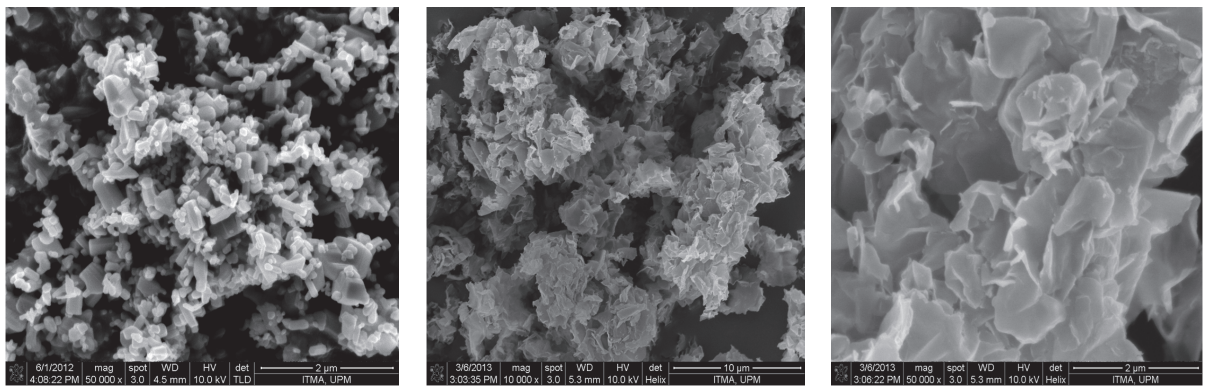

(a) (b) (c)

Figure 2: FESEM images of (a) ZnO at 50,000, (b) VAN at 10,000, and (c) VAN at 50,000 magnification.

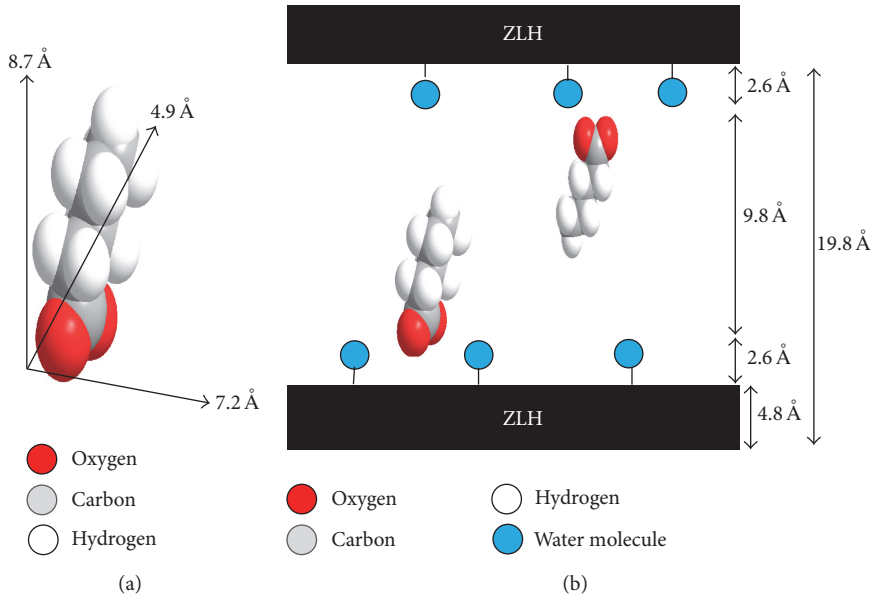

(a) (b)

Figure 3: (a) Three-dimensional molecular structure of VA and (b) spatial orientation of valerate in ZLH inorganic interspacing.

is observed for bands from CH_2 stretching and C-O asymmetric stretching which are shifted from 2964 to 2957 cm^{-1} and 1362 to 1370 cm^{-1}, respectively. The shift is due to the presence of VA anions between the host interspacings. On the other hand, the distinctive peak for C=O stretching vibration associated for COOH functional group [29] at 1712 cm^{-1} was not found in VAN spectrum. This C=O stretching band in valeric acid disappears after intercalation confirms that the anion was intercalated into ZLH layers which are in the anionic form of valeric acid, that is, valerate [29, 30]. A strong absorption band at 1545 cm^{-1} assigned for the antisymmetric carboxylate stretching indicates that there is an interaction between valerate anion and ZLH layers [30].

The presence of a broadband at 3380 cm^{-1} designated for OH group with O-H stretching vibration represents the adsorbed interlayer water [29]. ZnO band at the lower frequencies, 376 cm^{-1}, has subsided in VAN spectrum, suggesting that successful intercalation has occurred and all the ZnO has transformed into ZLH, resulting in the formation of VAN. The FTIR results which correspond with the PXRD pattern observed in Figure 1 supported the intercalation process of VA into the interlayer of zinc layered hydroxide.

4.4. Thermal Analysis. Figure 5 shows the TGA-DTG thermograms for pure ZnO, valeric acid, and VAN. For ZnO, a small weight loss of 0.4% was observed between 243.5 and 257.9°C with no maximum temperature indicating that this precursor is a very stable compound. A single weight loss of 99.3% was observed for valeric acid with maximum temperature occurring at 182.4°C compared to 207.6°C for VAN with weight loss of 15.5%. The decomposition temperature of VA intercalated inside the ZLH inorganic interlayer is higher compared to its counterpart anion. This suggests that the thermal stability of the VA in the nanohybrid is enhanced due to interaction with ZLH host. The intercalation process

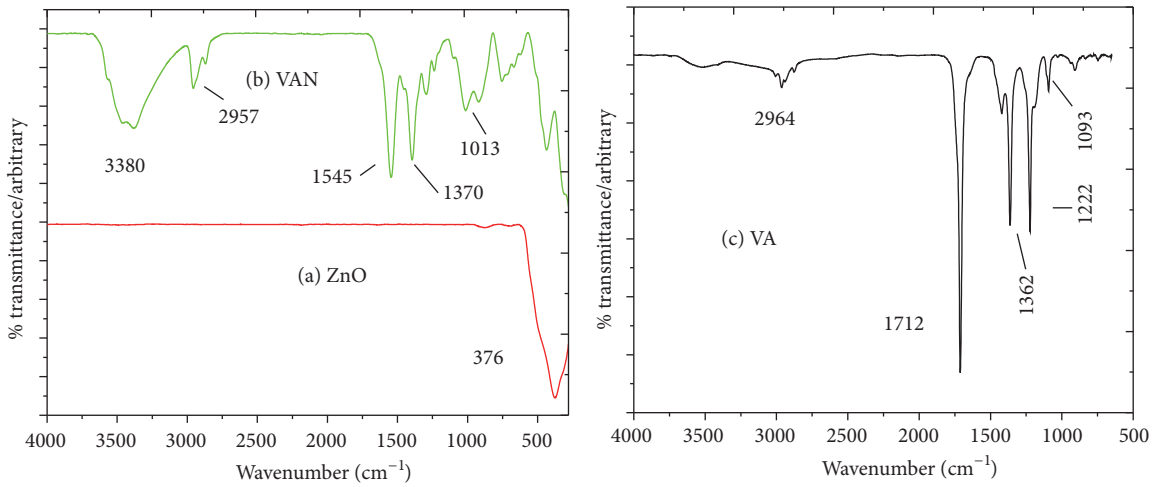

Figure 4: FTIR spectra of (a) ZnO, (b) VAN, and (c) ATR spectra of VA.

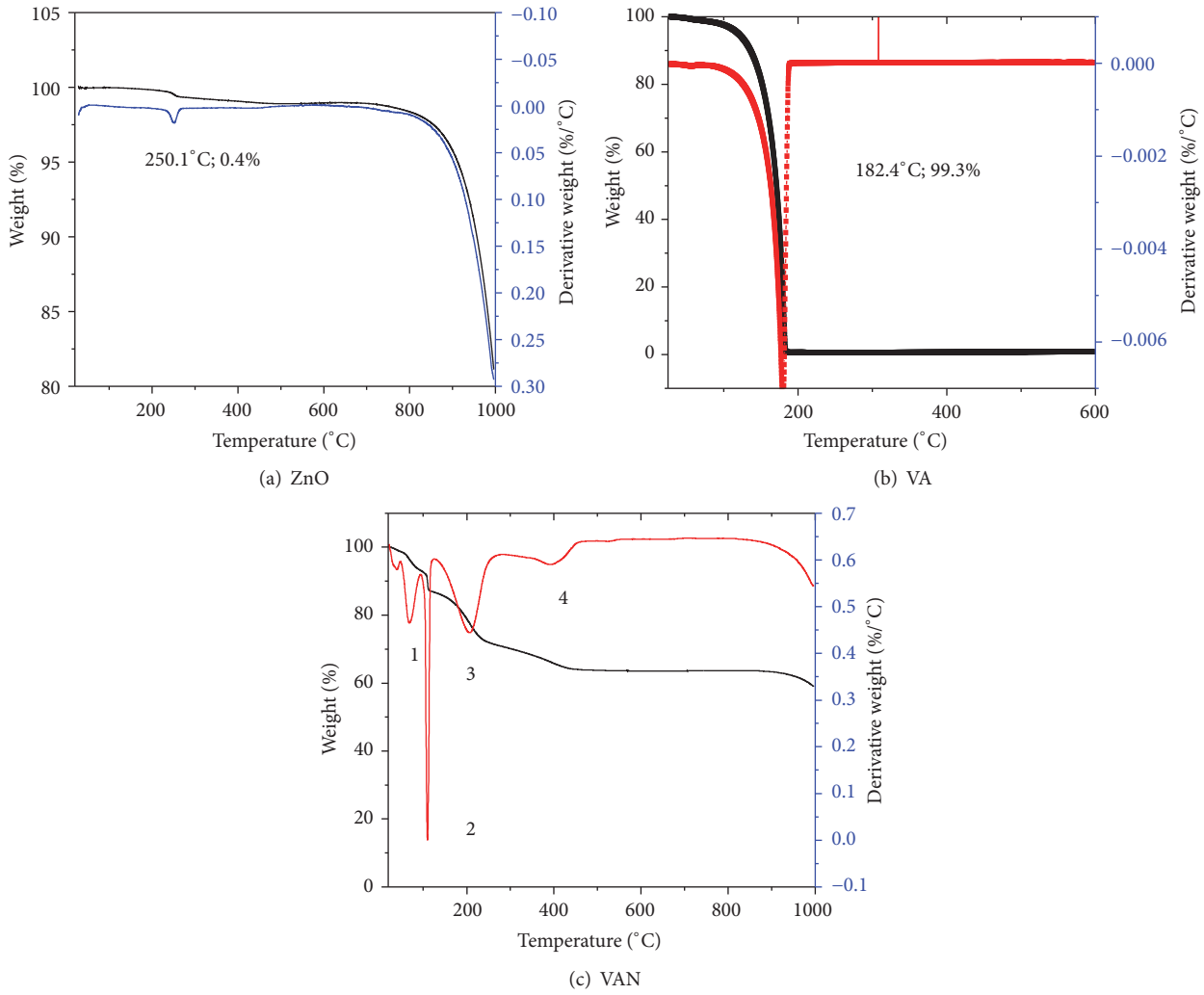

Figure 5: TGA-DTG thermograms of (a) ZnO, (b) VA, and (c) VAN.

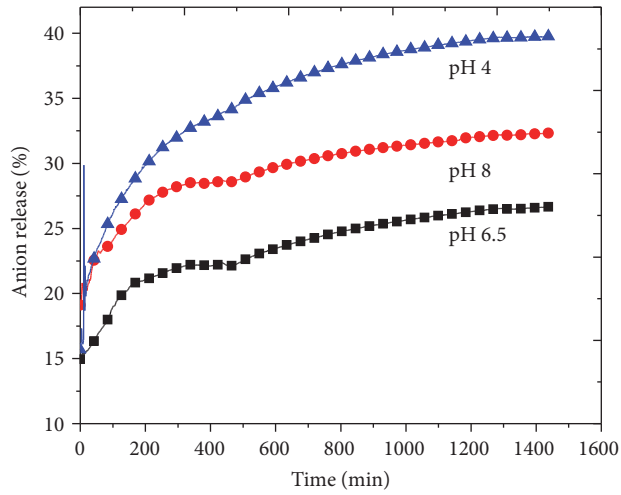

Figure 6: Release profiles of valeric acid from its nanohybrid, VAN interlayers into distilled water at pHs 4, 6.5, and 8.

Table 2: Maximum temperature and weight loss of VAN from TGA-DTG thermograms.

Peak	Maximum temperature (°C)	Weight loss (%)
1	37.4	5.5
2	111.8	6.4
3	207.6	15.5
4	399.2	6.4

Table 3: Chemical composition of VAN and percentage anion loading.

Sample	C (%w/w)	Zn (% w/w)	Anion loading (% w/w)
VAN	13.5	38.3	23.0

Table 4: Concentration of Zn (ppm) in the aqueous media at pH 4, pH 6.5, and pH 8.

	Aqueous media		
	pH 4	pH 6.5	pH 8
Content	19.91	5.15	11.32

resulted in the formation of electrostatic reaction between the guest anion and the inorganic ZLH layers [31].

The thermogram of VAN occurred in four stages of weight loss between 59.4 and 425.6°C. Table 2 reports on the maximum temperature and weight loss of VAN. The first two peaks of thermal decomposition were observed at temperature ranging from 59.4°C to 80.4°C and from 108.8°C to 111.2°C with weight loss of 5.5 and 6.4%, respectively. These weight losses are due to elimination of surface-physisorbed water and bonded water molecules [32].

The other stages of weight loss were contributed to the decomposition of organic moiety, VA anion, observed in 171.8–230.8°C region. The maximum temperature was detected at 207.6°C with corresponding weight loss of 15.5% due to the degradation of intercalated VA between the inorganic ZLH layers. The intercalated compound was further degraded to 6.4% at temperature range of 357.3–425.6°C. Further degradation occurs at temperature between 177.8 and 425.6°C with total weight loss of 21.9%. This result is close to the percentage anion loading of VA in VAN determined by CHNS, with a value of 23.0% as shown in Table 3. Chemical composition analysis (CHNS) revealed that VAN contained 13.5% carbon (w/w) which gave the percentage valerate anion loading in VAN nanohybrid calculated to be 23.0%. The percentage of valerate anion loading gave an indication of the degree of intercalation of guest anion in the ZLH host [29]. ICP-OES determination detected 38.3% (w/w) of Zn in VAN. Therefore, the formula of VAN was proposed as $Zn_{0.6}(OH)_{1.77}(CH_3CH_2CH_2CH_2COO^-)_{0.23}.0.66H_2O$.

4.5. Release Behavior of Valerate Anions. The controlled release study was carried out using distilled water at pHs 4, 6.5, and 8 to investigate the effect of different pH on the release behavior of valeric acid from ZLH intergallery. pH 4 and pH 8 were chosen to simulate the pH of acidic and alkaline soil. The release profiles of anion VA from the intergallery VAN into the release media are shown in Figure 6. The release rate of VA was found to be faster in the first 300 mins followed by a slower one, thereafter. In the first 300 mins, about 32, 22, and 28% of VA were released into pH 4, 6.5, and 8 aqueous solution, respectively. The fast release could be supported by the "burst effect" mechanism from the high release of adsorbed VA anions on the surface of inorganic layer ZLH [13]. Equilibrium stage was achieved after 1200 mins with maximum amount release recorded of 41, 27, and 33% in the pH 4, 6.5, and 8 aqueous solution, respectively.

The release rate of VA into the aqueous media can be arranged in the order of pH 4 > pH 8 > pH 6.5. Low and high pH of aqueous solution cause partial dissolution of ZLH due to the collapse of the inorganic layer structure [16] which resulted in the release of VA into the acidic and basic aqueous media. In this work, the aqueous solution of pH 4 and pH 8 contains 19.91 ppm and 11.32 ppm Zn^{2+}, respectively, as shown in Table 4. This implies that ZLH is not stable in low and high pHs and dissolution of the ZLH matrix affects the composition amount of VA released from the host, ZLH. ZLH which is more stable at pH 6.5 causes the release process of VA to be slower in comparison with the aqueous media at pH 4 and pH 8 aqueous media. The concentration of Zn^{2+} in the aqueous media at pH 6.5 after the controlled release is 5.15 ppm. It was found that the full release of VA did not happen as the saturated release was only achieved below 45%. This could be due to the strongly held VA anions by the positively charged layered host, resulting in the low release of VA into the aqueous solution [15].

4.6. Release Kinetics of Anions from VAN Intercalation Compound. To determine the release mechanism of VA from the nanohybrid, the controlled release data of VAN were fitted to several kinetic models, namely, pseudo-first order ($\ln(q_e - q_t) = \ln q_e - k_1 t$) [30] and pseudo-second order ($t/q_t = 1/k_2 q_e^2 + t/q_e$) [33] and parabolic diffusion ($(1 - M_t/M_o)/t = kt^{-0.5} + b$) [32], where q_e and q_t denote the equilibrium release amount and release amount of anion at

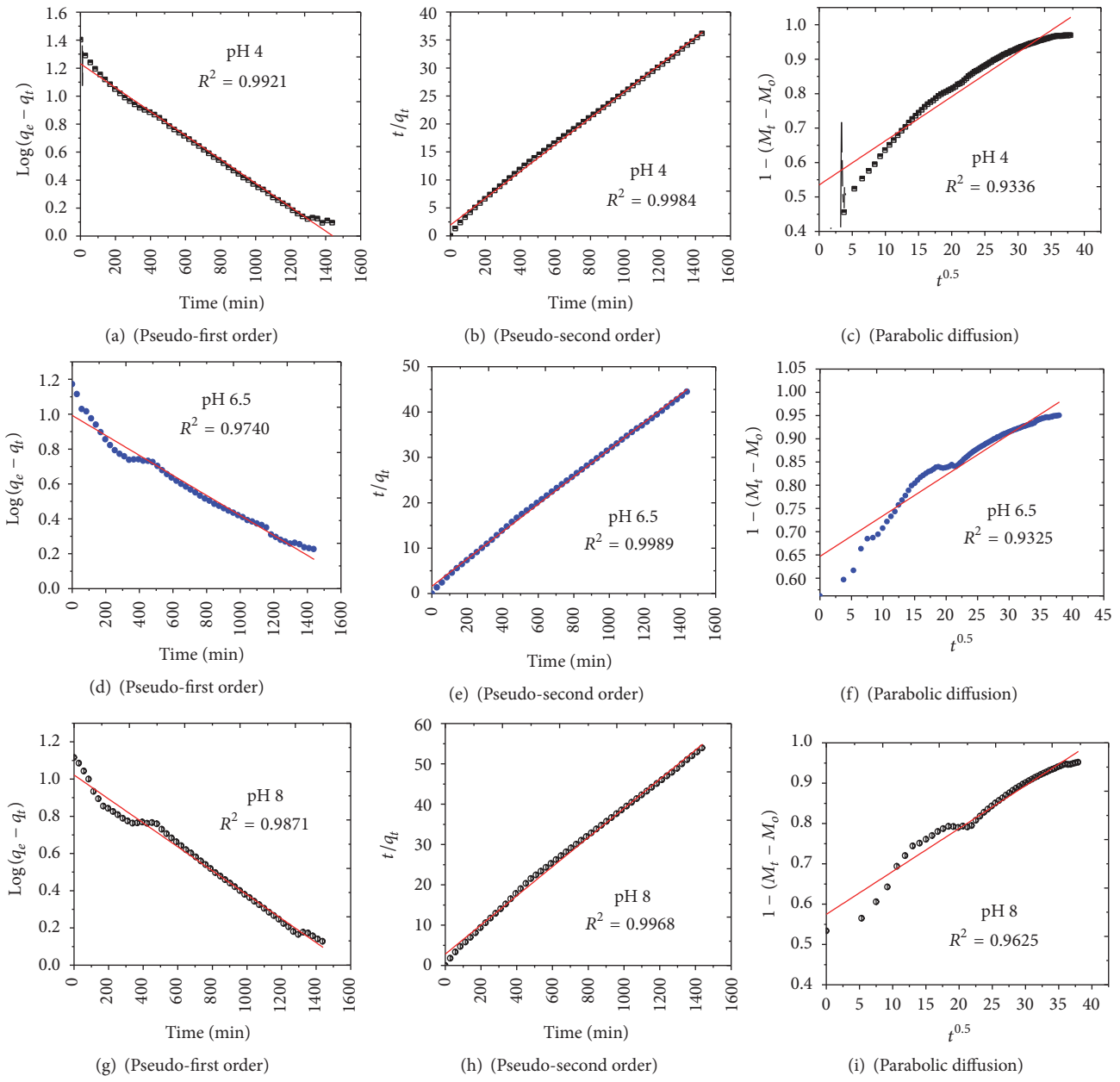

FIGURE 7: Fitting the data of valeric acid released from its intercalation compound into distilled water at different pHs using pseudo-first order and pseudo-second order and parabolic diffusion models at (a–c) pH 4, (d-e) pH 6.5, and (g–i) pH 8.

any time, t, respectively. k is the apparent release rate constant while M_o and M_t denote the anion remaining in the ZLH at zero time and release time, t, respectively. The corresponding linear correlation coefficient, r^2, value closest to 1, was used as a guide to the selection of the best fit kinetic model that describes the kinetic release of anion from VAN.

The pseudo-first order which describes the release is dependent on the dissolution of the host material, while the parabolic diffusion emphasizes on the diffusion-controlled process such as intraparticle diffusion or surface diffusion [34, 35]. Figure 7 shows plots of the fitting of valerate anions released from VAN while Table 5 reports on the results of fitting to the various kinetic models. The correlation coefficient, r^2, was found to be close to 1 when the data were fitted into pseudo-second-order kinetic model. This suggests that the release of valerate anion from the VAN was best expressed by the pseudo-second-order kinetic model. The release of valerate anion from the interlayer space is due to dissolution of VAN as well as ion exchange between valerate anions and the anions present in the aqueous media. In pH 4 and pH 8 solution, valerate anion was ion exchanged with Cl^- and OH^- due to the addition of HCL and NaOH, respectively [36]. In pH 6.5 solution, anion exchange between valerate ion and carbonate ion may occur due to the dissolution

Table 5: Parameters derived from the fitting of the data obtained from the release of VA from VAN intercalation compound into various pH solutions using parabolic diffusion, pseudo-first-order, and pseudo-second-order kinetic expression.

pH	Saturated release (%)	Correlation coefficient, r^2			Pseudo-second order
		Pseudo-first order	Pseudo-second order	Parabolic diffusion	Rate constant, k (mg/min) $\times 10^{-5}$
4	41	0.9921	**0.9984**	0.9336	2.49
6.5	27	0.9740	**0.9989**	0.9325	1.48
8	33	0.9871	**0.9968**	0.9625	1.87

of carbon dioxide from the atmosphere in distilled water [37]. The highest release rate value, k, of VA released into various pH media solutions is obtained in pH 4 media (2.49 $\times 10^{-5}$ mg/min) as shown in Table 5. This is agreeable to the highest saturated release values of 41% VA in pH 4 which suggested that the release of VA from intercalated compound into pH 4 is the fastest compared to pH 6.5 and pH 8. VA release from VAN into pH 6.5 solution has the lowest k rate that releases small amount of VA before equilibrium stage is achieved.

The release of VA from the intergallery of its organic-inorganic nanohybrid at various pHs was found to behave in a controlled manner governed by the pseudo-second-order kinetic rate expression. However, full release of VA into the release media was not achieved within the observed period, due to the strong electrostatic interaction of valerate anion and the positively charged ZLH interlayer, which affect the release process.

5. Conclusion

A new insect pheromone nanohybrid was successfully synthesized by the intercalation of valeric acid, a linear carboxylic group into ZLH interlayer via coprecipitation technique. The resulting nanohybrid material, VAN, has basal spacing of 19.8 Å without any ZnO peaks and implies full transformation of ZnO into the ZLH with bilayer arrangement of the guest anion between the host lattice spacings. The intercalation of VA into ZLH interlayer was supported by FTIR, ATR, and elemental analyses with percentage anion loading of 23.0% and the thermal stability of VA in the nanohybrid was enhanced compared to its counterpart anion. The release of VA anion from VAN behaved in a slow manner due to strong electrostatic interaction between the anion-host lattices governed by diffusion-anion exchange process. These findings provide the basis towards further development of organic-inorganic nanostructured material based on ZLH as host matrices for insect pheromone controlled release formulation.

Competing Interests

The authors declare that there are no competing interests regarding the publication of this paper.

Acknowledgments

This work was financially supported by the Ministry of Higher Education (MOHE) under Nanomite Grant no. 5526300. Sponsorship from Forest Research Institute Malaysia (FRIM) for Master Program for Rozita Ahmad is gratefully acknowledged.

References

[1] Advisory Committee on Pesticides, "Alternatives to Conventional Pest Control Techniques in the UK: a scoping study of the potential for their wider use," Advisory Committee on Pesticides (ACP), York, UK, Final Report of the Sub-group of the Advisory Committee on Pesticides, 2003.

[2] R. J. Petroski, M. R. Tellez, and R. W. Behle, *Semiochemicals in Pest and Weed Control: Anintroduction*, ACS Symposium Series, American Chemical Society, Washington, DC, USA, 2005.

[3] E. Touloupakis, A. Margelou, and D. F. Ghanotakis, "Intercalation of the herbicide atrazine in layered double hydroxides for controlled-release applications," *Pest Management Science*, vol. 67, no. 7, pp. 837–841, 2011.

[4] C. Nyambo, D. Chen, S. Su, and C. A. Wilkie, "Variation of benzyl anions in MgAl-layered double hydroxides: fire and thermal properties in PMMA," *Polymer Degradation and Stability*, vol. 94, no. 4, pp. 496–505, 2009.

[5] A. C. T. Cursino, J. E. F. D. C. Gardolinski, and F. Wypych, "Intercalation of anionic organic ultraviolet ray absorbers into layered zinc hydroxide nitrate," *Journal of Colloid and Interface Science*, vol. 347, no. 1, pp. 49–55, 2010.

[6] B. Li, J. He, D. G. Evans, and X. Duan, "Inorganic layered double hydroxides as a drug delivery system—intercalation and in vitro release of fenbufen," *Applied Clay Science*, vol. 27, no. 3-4, pp. 199–207, 2004.

[7] M. L. Zheludkevich, S. K. Poznyak, L. M. Rodrigues et al., "Active protection coatings with layered double hydroxide nanocontainers of corrosion inhibitor," *Corrosion Science*, vol. 52, no. 2, pp. 602–611, 2010.

[8] J.-M. Oh, T. T. Biswick, and J.-H. Choy, "Layered nanomaterials for green materials," *Journal of Materials Chemistry*, vol. 19, no. 17, pp. 2553–2563, 2009.

[9] T. W. Kim, S.-J. Hwang, Y. Park, W. Choi, and J.-H. Choy, "Chemical bonding character and physicochemical properties of mesoporous zinc oxide-layered titanate nanocomposites," *The Journal of Physical Chemistry C*, vol. 111, no. 4, pp. 1658–1664, 2007.

[10] C. Liang, Y. Shimizu, M. Masuda, T. Sasaki, and N. Koshizaki, "Preparation of layered zinc hydroxide/surfactant nanocomposite by pulsed-laser ablation in a liquid medium," *Chemistry of Materials*, vol. 16, no. 6, pp. 963–965, 2004.

[11] M. Fonrodona, J. Escarré, F. Villar et al., "PEN as substrate for new solar cell technologies," *Solar Energy Materials and Solar Cells*, vol. 89, no. 1, pp. 37–47, 2005.

[12] T. Hibino and H. Ohya, "Synthesis of crystalline layered double hydroxides: precipitation by using urea hydrolysis and subsequent hydrothermal reactions in aqueous solutions," *Applied Clay Science*, vol. 45, no. 3, pp. 123–132, 2009.

[13] A. Kasai and S. Fujihara, "Layered single-metal hydroxide/ethylene glycol as a new class of hybrid material," *Inorganic Chemistry*, vol. 45, no. 1, pp. 415–418, 2006.

[14] M. Ramli, M. Z. Hussein, and K. Yusoff, "Preparation and characterization of an anti-inflammatory agent based on a zinc-layered hydroxide-salicylate nanohybrid and its effect on viability of Vero-3 cells," *International Journal of Nanomedicine*, vol. 8, pp. 297–306, 2013.

[15] S. Jaerger, A. Zimmermann, S. F. Zawadzki, F. Wypych, and S. C. Amico, "Zinc layered hydroxide salts: intercalation and incorporation into low-density polyethylene," *Polimeros*, vol. 24, no. 6, pp. 673–682, 2014.

[16] M. Y. Ghotbi and M. Z. bin Hussein, "Gallate-Zn-Al-layered double hydroxide as an intercalated compound with new controlled release formulation of anticarcinogenic agent," *Journal of Physics and Chemistry of Solids*, vol. 71, no. 11, pp. 1565–1570, 2010.

[17] M. Z. Hussein, S. H. H. Al Ali, Z. Zainal, and M. N. Hakim, "Development of antiproliferative nanohybrid compound with controlled release property using ellagic acid as the active agent," *International Journal of Nanomedicine*, vol. 6, no. 1, pp. 1373–1383, 2011.

[18] A. M. Bashi, M. Z. Hussein, Z. Zainal, and D. Tichit, "Synthesis and controlled release properties of 2,4-dichlorophenoxy acetate-zinc layered hydroxide nanohybrid," *Journal of Solid State Chemistry*, vol. 203, pp. 19–24, 2013.

[19] T. Biswick, D.-H. Park, Y.-G. Shul, and J.-H. Choy, "P-coumaric acid-zinc basic salt nanohybrid for controlled release and sustained antioxidant activity," *Journal of Physics and Chemistry of Solids*, vol. 71, no. 4, pp. 647–649, 2010.

[20] A. C. T. Cursino, A. S. Mangrich, J. E. F. da Costa Gardolinski, N. Mattoso, and F. Wypych, "Effect of confinement of anionic organic ultraviolet ray absorbers into two-dimensional zinc hydroxide nitrate gallaries," *Journal of Brazilian Chemistry Society*, vol. 22, pp. 1183–1191, 2011.

[21] S. M. N. Mohsin, M. Z. Hussein, S. H. Sarijo, S. Fakurazi, P. Arulselvan, and T.-Y. Y. Hin, "Synthesis of (cinnamate-zinc layered hydroxide) intercalation compound for sunscreen application," *Chemistry Central Journal*, vol. 7, article 26, 2013.

[22] S. Inoue and S. Fujihara, "Liquid-liquid biphasic synthesis of layered zinc hydroxides intercalated with long-chain carboxylate ions and their conversion into ZnO nanostructures," *Inorganic Chemistry*, vol. 50, no. 8, pp. 3605–3612, 2011.

[23] A. Lenz, L. Selegård, F. Söderlind et al., "ZnO nanoparticles functionalized with organic acids: an experimental and quantum-chemical study," *The Journal of Physical Chemistry C*, vol. 113, no. 40, pp. 17332–17341, 2009.

[24] S. P. Newman and W. Jones, "Comparative study of some layered hydroxide salts containing exchangeable interlayer anions," *Journal of Solid State Chemistry*, vol. 148, no. 1, pp. 26–40, 1999.

[25] H. Nabipour and M. H. Sadr, "Controlled release of Diclofenac, an anti-inflammatory drug by nanocompositing with layered zinc hydroxide," *Journal of Porous Materials*, vol. 22, no. 2, pp. 447–454, 2015.

[26] M. Z. Hussein, N. Hashim, A. H. Yahaya, and Z. Zainal, "Synthesis and characterization of [4-(2,4-dichlorophenoxybutyrate)-zinc layered hydroxide] nanohybrid," *Solid State Sciences*, vol. 12, no. 5, pp. 770–775, 2010.

[27] F. Barahuie, M. Z. Hussein, P. Arulselvan, S. Fakurazi, and Z. Zainal, "Development of the anticancer potential of a chlorogenate-zinc layered hydroxide nanohybrid with controlled release property against various cancer cells," *Science of Advanced Materials*, vol. 5, no. 12, pp. 1983–1993, 2013.

[28] M. M. Bora, "Adsorption of pigment from annatto seed utilizing fish scale as biosorbent," *Journal of Chemistry Pharmacuetical Research*, vol. 2, no. 5, pp. 75–83, 2010.

[29] G. S. Machado, G. G. C. Arízaga, F. Wypych, and S. Nakagaki, "Immobilization of anionic metalloporphyrins on zinc hydroxide nitrate and study of an unusual catalytic activity," *Journal of Catalysis*, vol. 274, no. 2, pp. 130–141, 2010.

[30] B. Saifullah, M. Z. Hussein, S. H. Hussein-Al-Ali, P. Arulselvan, and S. Fakurazi, "Sustained release formulation of an anti-tuberculosis drug based on para-amino salicylic acid-zinc layered hydroxide nanocomposite," *Chemistry Central Journal*, vol. 7, article 72, 2013.

[31] S. H. Sarijo, M. Z. B. Hussein, A. H. Yahaya, Z. Zainal, and M. A. Yarmo, "Synthesis of phenoxyherbicides-intercalated layered double hydroxide nanohybrids and their controlled release property," *Current Nanoscience*, vol. 6, no. 2, pp. 199–205, 2010.

[32] F. Cavani, F. Trifirò, and A. Vaccari, "Hydrotalcite-type anionic clays: preparation, properties and applications," *Catalysis Today*, vol. 11, no. 2, pp. 173–301, 1991.

[33] J.-H. Yang, Y.-S. Han, M. Park, T. Park, S.-J. Hwang, and J.-H. Choy, "New inorganic-based drug delivery system of indole-3-acetic acid-layered metal hydroxide nanohybrids with controlled release rate," *Chemistry of Materials*, vol. 19, no. 10, pp. 2679–2685, 2007.

[34] M. Z. Hussein, N. F. B. Nazarudin, S. H. Sarijo, and M. A. Yarmo, "Synthesis of a layered organic-inorganic nanohybrid of 4-chlorophenoxyacetate-zinc-layered hydroxide with sustained release properties," *Journal of Nanomaterials*, vol. 2012, Article ID 860352, 9 pages, 2012.

[35] T. Kodama, Y. Harada, M. Ueda, K.-I. Shimizu, K. Shuto, and S. Komarneni, "Selective exchange and fixation of strontium ions with ultrafine Na-4-mica," *Langmuir*, vol. 17, no. 16, pp. 4881–4886, 2001.

[36] S. S. D. Richardson-Chong, R. Patel, and G. R. Williams, "Intercalation and controlled release of bioactive ions using a hydroxy double salt," *Industrial and Engineering Chemistry Research*, vol. 51, no. 7, pp. 2913–2921, 2012.

[37] S.-J. Xia, Z.-M. Ni, Q. Xu, B.-X. Hu, and J. Hu, "Layered double hydroxides as supports for intercalation and sustained release of antihypertensive drugs," *Journal of Solid State Chemistry*, vol. 181, no. 10, pp. 2610–2619, 2008.